Available online at www.sciencedirect.com
ScienceDirect
Journal of Organometallic Chemistry 692 (2007) 4760–4767
Journal of Organometallic Chemistry
www.elsevier.com/locate/jorganchem

A unique coplanar multi-center bonding network in doubly acetylide-bridged binuclear zirconocene complexes: A density functional theory study

Shuqiang Niu [a,*], Agnes Derecskei-Kovacs [b,1], Michael B. Hall [b,*]

[a] Department of Chemistry, Georgetown University, Washington, DC 20057-1227, United States
[b] Department of Chemistry, Texas A&M University, College Station, TX 77843, United States

Received 24 April 2007; received in revised form 7 July 2007; accepted 7 July 2007
Available online 25 July 2007

Abstract

A unique π-conjugative interaction pattern was experimentally revealed in the doubly acetylide-bridged binuclear group 4 metallocene complexes, which was involved in C–C coupling/cleavage reactions of acetylides and σ-alkynyl migrations. To elucidate how this multi-center bonding network affects the structural and reaction properties of these complexes, density functional theory (DFT) calculations and molecular orbital (MO) analysis were carried out on the electronic structure and σ-alkynyl migration mechanisms of the doubly acetylide-bridged binuclear Zr complexes, $(L_2Zr)_2(\mu\text{-}C{\equiv}CH)_2$ (L = Cp, Cl). The B3LYP calculations suggested that the doubly [σ,π] acetylide-bridged complex C_{2h}-$(L_2Zr)_2(\mu\text{-}C{\equiv}CH)_2$ was produced by the reaction of $L_2Zr(C{\equiv}CH)_2$ with L_2Zr through a C_{2v}-$(L_2Zr)_2(\mu\text{-}C{\equiv}CH)_2$ intermediate followed by an isomerization process. In particular, the isomerization of C_{2h}- or C_{2v}-$(L_2Zr)_2(\mu\text{-}C{\equiv}CH)_2$ is almost thermoneutral through a low barrier of 15.3–17.0 kcal/mol. The MO Walsh diagram revealed that the two isomers have a very similar six-center-six-electron bonding network. The coplanar π-conjunctive interaction by the electron donating and back-donating interactions between the metal centers and acetylide ligands significantly stabilizes the doubly acetylide-bridged binuclear group 4 metallocene complexes and the isomerization transition state.

Keywords: Density functional theory; C–C coupling; Coplanar multi-center bonding; Alkynyl migration mechanism; Isomerization transition state

1. Introduction

As elementary steps in homogeneous catalysis processes, the C–C coupling reactions mediated by early transition metal complexes have become one of most attractive areas in studies of oligomerizations and polymerizations of alkenes and alkynes [1,2]. Generally, the C–C coupling of alkene or alkyne insertion into M–R bonds (M = group 4 d^0 transition metals; R = alkyl) is achieved by multi-center σ-bonding interactions which significantly stabilize the insertion transition state and product, resulting in lower activation and reaction energies [3]. As shown in Scheme 1, when the inserted molecule adjoins the d^0 M center, the coplanar π-orbital electrons tend to be polarized towards $C_\alpha^{\delta-}$–$C_\beta^{\delta+}$ followed by electron migration of M–R to C_β, ultimately forming a four-center, four-electron bonding pattern (a) in the insertion transition state and a three-center two-electron bonding pattern (b) in the insertion product [3–5]. Similar multi-center bonding patterns have been also characterized in a number of group 4 d^0 metallocene complexes, including those β/γ-agostic complexes and dinuclear complexes with a planar tetracoordinate carbon center (Scheme 1c) [6–10]. Apparently,

* Corresponding authors. Tel.: +1 202 687 5557; fax: +1 202 687 6209 (S. Niu).
E-mail addresses: sn72@georgetown.edu (S. Niu), hall@science.tamu.edu (M.B. Hall).
[1] Current address: Research Center, Millennium Chemicals, United States.

0022-328X/$ - see front matter © 2007 Elsevier B.V. All rights reserved.
doi:10.1016/j.jorganchem.2007.07.019

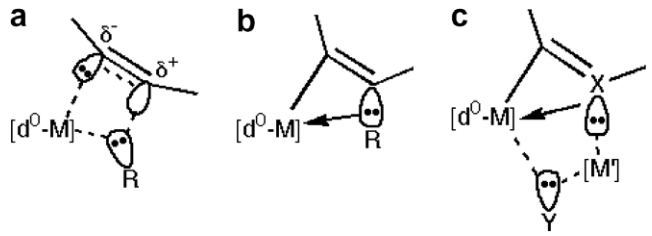

Scheme 1.

the strongly electrophilic nature of group 4 d^0 metallocene center plays a critical role as an electron "transit" center throughout the alkene or alkyne insertion processes since it not only tunes energies of the coupled carbon orbitals, but also provides extra stabilizing force for the carbon network during bond rearrangement processes.

In addition, a unique π-conjugative interaction pattern was revealed in the group 4 doubly acetylide-bridged binuclear metallocene complexes, which were involved in C–C coupling/cleavage reactions acetylides [11–31]. These doubly acetylide-bridged binuclear complexes $(Cp_2M)_2(\mu\text{-}C{\equiv}CR)_2$ (M = Ti, Zr; Cp = η^5-cyclopentadienyl) can be obtained either by reacting $Cp_2M(C{\equiv}CR)_2$ with "Cp_2M" or by reacting $RC{\equiv}C\text{–}C{\equiv}CR$ with "Cp_2M" [32]. The X-ray crystal structure analysis showed that these complexes generally adopt a C_{2h}-symmetric molecular structure, in which the central $(Cp_2M)_2$ core atoms conjugated with the four acetylide ligand carbon atoms as shown in Scheme 2a. A unique geometric character of the C_{2h}-$(Cp_2M)_2(\mu\text{-}C{\equiv}CR)_2$ is that the M–C_α bonds are significantly shorter while the C_α–C_β bonds are longer than those of $Cp_2M(C{\equiv}CR)_2$. Erker and coworkers suggested that these very characteristic structural parameters might be attributed to a considerable π-interaction between the metal centers and the adjacent organic π-system across the connecting σ-bond [33]. Furthermore, an intramolecular σ-alkynyl migration has been observed for the binuclear Zr complexes at higher temperature by NMR spectra. The resulted regioisomer has a C_{2v}-symmetric $(Cp_2M)_2(\mu\text{-}C{\equiv}CR)_2$ structure (Scheme 2b) [33]. Although the C_{2v}-isomer appears to be a "mixed-valence" Zr(IV)–Zr(II) complex, it is only slightly less stable by ~0.1 kcal/mol than its C_{2h}-$(Cp_2M)_2(\mu\text{-}C{\equiv}CR)_2$ isomer [33]. Since the C_{2v}-isomer was not observed by X-ray crystallography, the detailed structural differences are unclear between the C_{2h}- and C_{2v}-isomers. Moreover, although many highly symmetric binuclear doubly acetylide-bridged complexes have been reported (Scheme 2c) [11,33], the isomerization between the C_{2h}- and C_{2v}-isomers and the automerization of the C_{2h}- and C_{2v}-isomers through the D_{2h}-binuclear complexes in the σ-alkynyl migration processes still remain uncertain.

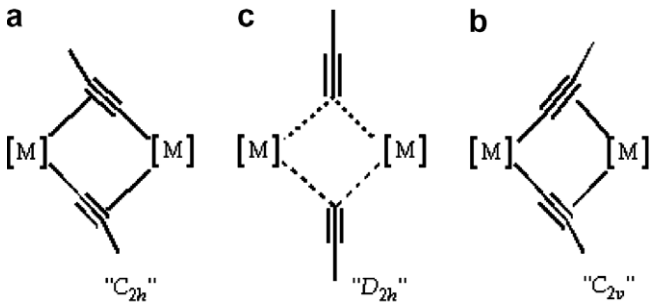

Scheme 2.

Computational chemistry has become powerful technique in studying the structures, electronic structures, and reaction mechanisms of real molecular systems containing transition metals [3]. The aim of this work is to explore the bonding and σ-alkynyl migration mechanism of the doubly acetylide-bridged binuclear Zr complexes using the density functional theory (DFT) calculations and molecular orbital (MO) analysis. The computational results are compared with the X-ray crystal structures and the results of temperature-dependent dynamic NMR spectra. The current theoretical study may provide useful information in understanding the functions of the multicenter bonding network in the group 4 doubly acetylide-bridged binuclear metallocene complexes as well as related catalytic processes.

2. Computational details

Two molecular models were utilized in this study. As distinct from the full molecular model (Model 1), the Cp rings of the binuclear Zr complexes were replaced by the chloride atoms in the simplified model (Model 2). Model 2 generally gave reasonable descriptions of the related electronic structures and reaction properties of alkylzirconocenes [3,34], and thus is suitable for both geometry and reaction energy calculations of zirconocene systems without significant steric influence (*vide infra*).

The DFT functional [35], specifically with the Becke's three-parameter hybrid exchange functional [36] and the Lee–Yang–Parr correlation functional (B3LYP) [37], was utilized for the geometry optimizations, electronic structure calculations, and energetic calculations of the doubly acetylide-bridged binuclear Zr complexes. The basis set for Zr is a modified version of LANL2DZ basis set by Couty and Hall [38–41], where the two outermost p functions of Zr was replaced by a [41] split of the optimized 5p function. For carbon and hydrogen atoms, two different sets of basis sets were used in calculations of Models 1 and 2, respectively. In Model 1, the standard LANL2DZ basis sets [42] were used for carbon and hydrogen atoms of the bridged alkynyl ligands, whereas the STO-3G basis sets [43] were used for atoms of the Cp ring. In Model 2, the standard LANL2DZ basis set was used for chloride, carbon, and hydrogen atoms of the complexes. Transition states (TS) were optimized by the Berny algorithm [44], in which the final updated Hessian shows only one negative eigenvalue. All possible transition structures were further characterized by determining the number of imaginary frequencies [45].

All geometric and energetic calculations were performed using the GAUSSIAN98 program [46]. The molecular orbital calculations and visualizations were performed using the NWChem [47,48] and extensible computational chemistry environment (Ecce) application software [49].

3. Results and discussion

3.1. Bonding properties of mononuclear σ-alkynyl Zr complexes

To explore the bonding properties of the doubly acetylide-bridged binuclear Zr complexes, a comparison is first made here between the mononuclear complexes $L_2Zr(CH_3)_2$ and $L_2Zr(C{\equiv}CH)_2$ (L = Cp, Cl). The B3LYP optimized geometries of $L_2Zr(CH_3)_2$ and $L_2Zr(C{\equiv}CH)_2$ (L = Cp, Cl) are shown in Table 1. In comparison to the experimental geometric parameters [33,50], the calculations using Model 1 gave excellent description of bond lengths and bond angles of $L_2Zr(CH_3)_2$ and $L_2Zr(C{\equiv}CH)_2$ but a longer $C_\alpha{\equiv}C_\beta$ bond length by ~0.04 Å. Although the calculations using Model 2 gave shorter Zr–C_α and $C_\alpha{\equiv}C_\beta$ bond lengths as well as larger C_α–Zr–$C_{\alpha'}$ bond angle relative to those using Model 1, the calculations using Model 2 give reasonable description of changes in these bond lengths and bond angles between $L_2Zr(CH_3)_2$ and $L_2Zr(C{\equiv}CH)_2$.

In comparison to $L_2Zr(CH_3)_2$, the calculated Zr–C_α and Zr–L bond lengths of $L_2Zr(C{\equiv}CH)_2$ decrease by about 0.05 and 0.02 Å, respectively, whereas the C_α–Zr–$C_{\alpha'}$ angle significantly increases by about 4°, in very good agreement with the experimental values. Although the changes in geometry of $L_2Zr(C{\equiv}CH)_2$ may be attributed to the better electron donor properties of acetylide and the stronger Coulomb repulsion between acetylides, the longer C_α–C_β bond length of 0.02 Å of $L_2Zr(C{\equiv}CH)_2$ relative to 1.222 Å of an acetylide molecule at the B3LYP/LANL2DZ level implies π-conjugation between the Zr and the alkynyl ligands. The MO analysis revealed that the slight π-conjugations occur in the $(\pi_{\|} + \pi_{\|})$ and $(\pi_{\perp} - \pi_{\perp})$ orbitals of $L_2Zr(C{\equiv}CH)_2$ (Fig. 1).

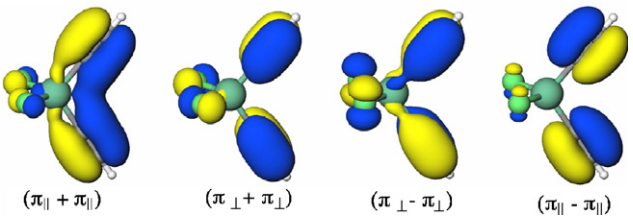

Fig. 1. The calculated π MO orbitals of $Cl_2Zr(\mu\text{-}C{\equiv}CR)_2$.

3.2. Bonding and energetic properties of doubly acetylide-bridged binuclear Zr complexes

Experimentally, the bis(σ-alkynyl)zirconocene complexes $Cp'_2Zr(C{\equiv}CR)_2$ can react with (butadiene)zirconocenes "Cp'_2Zr" to produce doubly acetylide-bridged binuclear Zr complexes $(Cp'_2Zr)_2(\mu\text{-}C{\equiv}CR)_2$ [12,33]. Although the X-ray crystal structure analysis and the low-temperature NMR spectra revealed that the binuclear Zr complexes adopted a C_{2h}-symmetric molecular structure, in which two identical $Cp'_2Zr(C{\equiv}CR)$ units appear to have dimerized, the $[\sigma,\sigma][\pi,\pi]$-acetylide-bridged $(Cp'_2Zr)_2(\mu\text{-}C{\equiv}CR)_2$ with C_{2v} symmetry observed by the higher-temperature NMR spectra may be the expected initial doubly acetylide-bridged binuclear Zr product. The low isomerization energy of ~0.1 kcal/mol between the C_{2h}- and C_{2v}-isomers evaluated by the variable-temperature NMR experiments implied the high similarity between two isomers in their overall electronic structure. To elucidate bonding properties of the doubly acetylide-bridged binuclear Zr complexes, we calculated geometric parameters of the C_{2h}- and C_{2v}-isomers, and compared mono- and binuclear Zr complexes. The B3LYP optimized geometries of $(L_2Zr)_2(\mu\text{-}C{\equiv}CH)_2$ (L = Cp, Cl) are shown in Fig. 2 and Table 2.

Our calculations revealed that although the L_2Zr species theoretically favors a triplet state in the gas phase, the binuclear complexes $(L_2Zr)_2(\mu\text{-}C{\equiv}CH)_2$ exhibit a singlet ground state, which is more stable by over 40 kcal/mol than the triplet state. Furthermore, broken-symmetry DFT calculations show that as L_2Zr approachs to $(L_2Zr)_2(\mu\text{-}C{\equiv}CH)_2$, the spin densities of the spin coupled

Table 1
The B3LYP calculated and experimental geometric parameters (bond length in Å and bond angle in °) of $L_2Zr(CH_3)_2$ and $L_2Zr(C{\equiv}CH)_2$ (L = Cp, Cl)

	$L_2Zr(CH_3)_2$			$L_2Zr(C{\equiv}CH)_2$		
	Model 1[a]	Model 2[b]	Experimental[c]	Model 1	Model 2	Experimental[d]
Zr–C_α	2.300	2.200	2.270	2.244	2.150	2.249
Zr–L	2.254	2.416	2.23	2.234	2.398	2.211
C_α–C_β				1.244	1.242	1.206
L–Zr–L	135.6	120.0	132.5	135.5	112.2	132.6
C_α–Zr–$C_{\alpha'}$	96.6	102.8	95.6	101.7	106.6	103.6

[a] L = Cp.
[b] L = Cl.
[c] Ref. [50].
[d] Ref. [33].

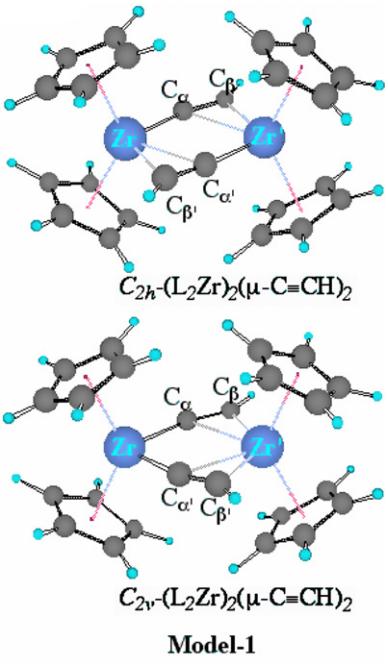

Fig. 2. The B3LYP optimized geometries of $(L_2Zr)_2(\mu\text{-}C{\equiv}CH)_2$ using Model 1 (L = Cp).

wavefunction of $(L_2Zr)_2(\mu\text{-}C{\equiv}CH)_2$ always vanish. This result implies that the two d electrons significantly delocalize between the two fragments toward a normal covalence bonding interaction. In the C_{2v}-$(L_2Zr)_2(\mu\text{-}C{\equiv}CH)_2$ isomer, the L_2Zr species directly coordinates with both of acetylides of $L_2Zr(C{\equiv}CH)_2$, resulting in a dramatic decrease of 10–16° in the C_α–Zr–$C_{\alpha'}$ bond angle. The π-type Zr–$C_{\alpha'}$/$C_{\beta'}$ distances of C_{2v}-$(L_2Zr)_2(\mu\text{-}C{\equiv}CH)_2$ are about 2.30–2.61 Å, whereas the σ-type Zr–C_α bond lengths are about 2.13–2.19 Å, revealing a typical character of the coplanar $[\sigma,\sigma][\pi,\pi]$ acetylide-bridged complex. In particular, the π-type Zr–$C_{\beta'}$ bond length is closer to the Zr–C bond length of $L_2Zr(CH_3)_2$, showing a significant σ Zr–C bonding character. In comparison to $L_2Zr(C{\equiv}CH)_2$, the σ-type Zr–C bond lengths of C_{2v}-$(L_2Zr)_2(\mu\text{-}C{\equiv}CH)_2$ are shorter by 0.02–0.05 Å and the C_α–C_β bonds are longer by 0.01–0.05 Å, exhibiting more bonding interaction between the Zr and the alkynyl ligands relative to a typical Zr–C_α σ-bond. Since only two d electrons of the L_2Zr species and four coplanar π-electrons of the alkynyl ligands of $L_2Zr(C{\equiv}CH)_2$ are involved in these additional bonding interaction, these bonding interactions appear to be consequence of a unique multi-center bonding network. The MO analysis provides unambiguous interpretation for this unique bonding network structure. The left of Fig. 3 exhibits three orbitals occupied by six electrons involved in the multi-center bonding interaction of C_{2v}-$(L_2Zr)_2(\mu\text{-}C{\equiv}CH)_2$. As expected, the $(\pi_\| + \pi_\|)$ and $(\pi_\| - \pi_\|)$ orbitals of $L_2Zr(C{\equiv}CH)_2$ interact with the unoccupied d_{z^2} and d_{xy} orbitals of L_2Zr to form two three-center-two-electron bonds. It is worthy to note that a unique bonding interaction occurs in the highest occupied molecular orbital (HOMO) of C_{2v}-$(L_2Zr)_2(\mu\text{-}C{\equiv}CH)_2$ arising from the interaction of the occupied $d_{x^2-y^2}$ orbital of the L_2Zr unit with the unoccupied $(\pi^*_\| + \pi^*_\|)$ and $d_{x^2-y^2}$ orbitals of $L_2Zr(C{\equiv}CH)_2$. This significant bonding interaction leads to electron density of L_2Zr back donating to $L_2Zr(C{\equiv}CH)_2$, consequently generating either a Zr–C_β bond or a Zr=C_α bond and resulting in an additional stabilizing force. Therefore, the multi-center bonding network of C_{2v}-$(L_2Zr)_2(\mu\text{-}C{\equiv}CH)_2$ can be represented by resonance formula A, B, B′, C, and C′ in Scheme 3, in which six electrons delocalize among two Zr and four carbon atoms.

The coplanar $[\sigma,\pi][\sigma,\pi]$-acetylide-bridged isomer, C_{2h}-$(L_2Zr)_2(\mu\text{-}C{\equiv}CH)_2$, can be generated by intramolecular σ-alkynyl migration of C_{2v}-$(L_2Zr)_2(\mu\text{-}C{\equiv}CH)_2$. The DFT calculations using both of Models 1 and 2 give reasonable descriptions of the geometric structure in comparison to the X-ray crystal structure of C_{2h}-$(Cp_2Zr)_2(\mu\text{-}C{\equiv}CR)_2$ [12]. In comparison to the C_{2v}-isomer, the σ-type Zr–C_α bond lengths and the π-type Zr–C_β distances of C_{2h}-

Table 2
The B3LYP calculated geometric parameters (bond length in Å and bond angle in °) of the C_{2v}- and C_{2h}-$(L_2Zr)_2(\mu\text{-}C{\equiv}CH)_2$ (L = Cp, Cl)

	C_{2v}-$(L_2Zr)_2(\mu\text{-}C{\equiv}CH)_2$			C_{2h}-$(L_2Zr)_2(\mu\text{-}C{\equiv}CH)_2$		
	Model 1[a]	Model 2[b]	Experimental	Model 1	Model 2	Experimental[c]
Zr–Zr′	3.623	3.524		3.600	3.472	3.505
Zr–C_α	2.193	2.131		2.198	2.142	2.187
Zr–$C_{\alpha'}$	2.613	2.494		2.545	2.418	2.431
Zr–$C_{\beta'}$	2.438	2.298		2.413	2.305	2.405
Zr–L	2.300	2.409		2.309	2.409	2.255
Zr′–L	2.316	2.406		2.309	2.409	2.255
C_α–C_β	1.258	1.287		1.264	1.291	1.260
Zr–C_α–C_β	165.3	165.0		167.9	168.3	172.3
C_α–C_β–H	148.4	147.0		147.0	147.0	146.8
L–Zr–L	131.8	122.5		129.6	118.5	128.0
L–Zr′–L	128.3	114.5		129.6	118.5	128.0
C_α–Zr–$C_{\alpha'}$	91.2	88.7		81.5	81.0	81.4

[a] L = Cp.
[b] L = Cl.
[c] Ref. [12].

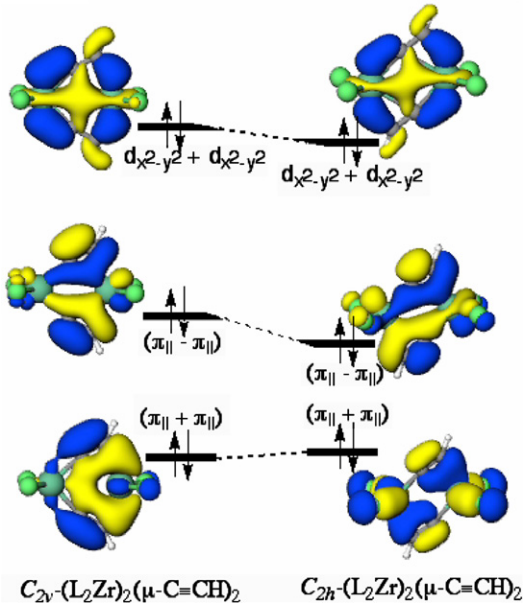

Fig. 3. The schematic MO Walsh diagrams calculated coplanar π MO orbitals for the C_{2v}- to C_{2h}-$(L_2Zr)_2(\mu\text{-}C{\equiv}CH)_2$ isomers.

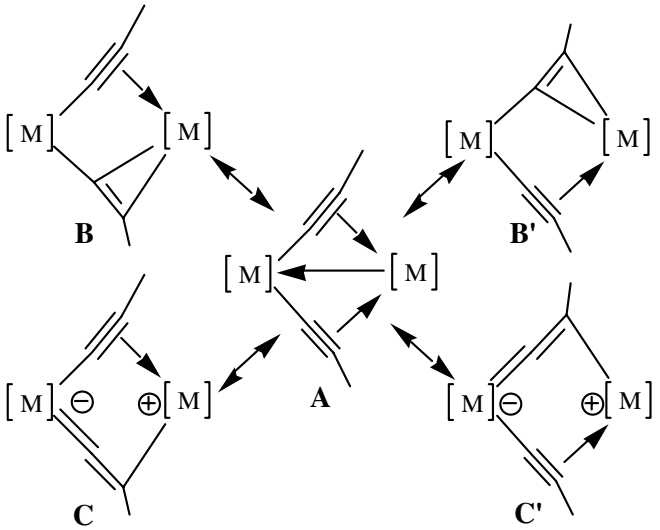

Scheme 3.

$(L_2Zr)_2(\mu\text{-}C{\equiv}CH)_2$ change only slightly by less than 0.01 Å, whereas the π-type Zr–C_α distances are significantly shorter by about 0.07 Å. Thus, the bonding interactions between the Zr sites and alkynyl ligands in the C_{2h}-isomer increase. On the other hand, the shorter Zr–Zr distance and the smaller difference between the π-type Zr–C_α and Zr–C_β distances relative to the C_{2v}-isomer indicates that the two $(L_2Zr)(C{\equiv}CH)$ moieties bond each other more strongly than the L_2Zr and $L_2Zr(C{\equiv}CH)_2$ moieties because of smaller steric influence. The further MO analysis reveals that C_{2h}-$(Cp_2Zr)_2(\mu\text{-}C{\equiv}CR)_2$ is similar to the C_{2v}-isomer in multi-center bonding properties. The occupied ($\pi_{\|} + \pi_{\|}$) and ($\pi_{\|} - \pi_{\|}$) orbitals of the $L_2Zr(C{\equiv}CH)$ unit interact with the unoccupied d_{z^2} and d_{xy} orbitals of another $L_2Zr(C{\equiv}CH)$ unit to form two sets of three-center-two-electron bonds, while two HOMO electrons delocalize on the ($\pi^*_{\|} + \pi^*_{\|}$) orbitals of alkynyl ligands and the $d_{x^2-y^2}$ orbitals of $L_2Zr(C{\equiv}CH)$ units to form either a Zr–C_β/C_β bond or a Zr=C_α bond (Fig. 3). Therefore, a similar multi-center bonding network can be also represented by resonance formula A, B, B′, C, and C′ in Scheme 4, in which six electrons delocalize among two Zr and four carbon atoms of C_{2h}-$(L_2Zr)_2(\mu\text{-}C{\equiv}CH)_2$.

Since both the $(L_2Zr)_2(\mu\text{-}C{\equiv}CH)_2$ isomers exhibit a similar multi-center bonding network structure, the energy difference between two isomers should be very small. The B3LYP/LANL2DZ calculations suggest that the isomerization energy of C_{2v}- to C_{2h}-$(L_2Zr)_2(\mu\text{-}C{\equiv}CH)_2$ in gas phase is only −1.88 kcal/mol for Model 1 and −2.77 kcal/mol for Model 2. The isomerization free energy at 300 K is −1.70 kcal/mol for Model 1. These results support the C_{2h}-$(L_2Zr)_2(\mu\text{-}C{\equiv}CH)_2$ isomer as the major product at room temperature. On the other hand, we have noted that the intramolecular σ-alkynyl migration of C_{2v}-$(L_2Zr)_2(\mu\text{-}C{\equiv}CH)_2$ to the C_{2h}-isomer leads to a decrease of about 0.6 cal/mol K in entropy. Thus, with an increase in temperature the C_{2v}-$(L_2Zr)_2(\mu\text{-}C{\equiv}CH)_2$ may be thermodynamically favored over the C_{2h}-isomer. Overall, the experimental process appears to proceed along the reaction of $Cp'_2Zr(C{\equiv}CR)_2$ with Cp'_2Zr through the C_{2v}-$(Cp'_2Zr)_2$-$(\mu\text{-}C{\equiv}CH)_2$ isomer to generate a C_{2h}-$(Cp'_2Zr)_2(\mu\text{-}C{\equiv}CH)_2$ complex at lower temperature, which is possibly followed by a reversed reaction to give the C_{2v}-$(L_2Zr)_2(\mu\text{-}C{\equiv}CH)_2$ isomer at higher temperature. To support this assumption, we further calculate the possible isomerization and automerization processes of $(L_2Zr)_2(\mu\text{-}C{\equiv}CH)_2$.

3.3. Isomerization and automerization of doubly acetylide-bridged binuclear Zr complexes

Since the higher symmetry D_{2h}-$(L_2M)_2(\mu\text{-}C{\equiv}CR)_2$ complexes have been proposed to be involved in isomerization

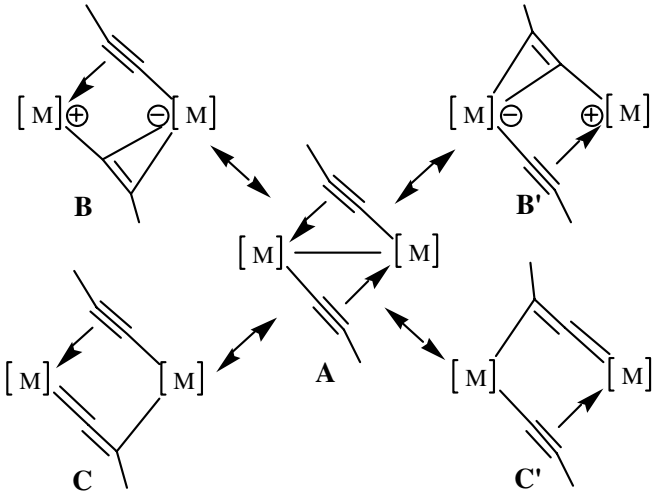

Scheme 4.

of the doubly acetylide-bridged binuclear complexes, the automerization of C_{2v}- and C_{2h}-$(L_2Zr)_2(\mu\text{-}C{\equiv}CH)_2$ may proceed via either the D_{2h}-$(L_2Zr)_2(\mu\text{-}C{\equiv}CH)_2$ species or their isomerizations. Here, our focus is on the possible role of a D_{2h}-$(L_2Zr)_2(\mu\text{-}C{\equiv}CH)_2$ intermediate and the isomerization transition state of C_{2v}- to C_{2h}-$(L_2Zr)_2(\mu\text{-}C{\equiv}CH)_2$.

The geometry optimization without symmetry restriction failed to converge to the D_{2h}-$(L_2Zr)_2(\mu\text{-}C{\equiv}CH)_2$ (L = Cp, Cl) species, and led toward either C_{2v}- or C_{2h}-$(L_2Zr)_2(\mu\text{-}C{\equiv}CH)_2$ complex. The Hessian analysis along the transition state optimization revealed that two negative eigenvalues occur around the D_{2h}-$(L_2Zr)_2(\mu\text{-}C{\equiv}CH)_2$ structure. To verify stationary properties of the D_{2h}-$(L_2Zr)_2(\mu\text{-}C{\equiv}CH)_2$ species, the restricted symmetric optimization followed by frequency calculation is carried out on this structure. The B3LYP calculations reveal that the D_{2h}-$(L_2Zr)_2(\mu\text{-}C{\equiv}CH)_2$ species (Fig. 5) has two imaginary frequencies at -316 and $-224\ cm^{-1}$, which are related to two alkynyl ligand migrations, and is higher by 56.5 kcal/mol in energy than the C_{2h}-$(L_2Zr)_2(\mu\text{-}C{\equiv}CH)_2$ complex. These results confirm that the D_{2h}-$(L_2Zr)_2(\mu\text{-}C{\equiv}CH)_2$ species is not a transition state but a second order saddle point on the potential energy surface which links the C_{2v}- and C_{2h}-$(L_2Zr)_2(\mu\text{-}C{\equiv}CH)_2$ isomers (Fig. 4).

Moreover, a transition state is found by a transition state search from the C_{2v}-$(L_2Zr)_2(\mu\text{-}C{\equiv}CH)_2$ to the C_{2h}-isomer, in which only one σ-alkynyl ligand shifts from one metal center to the another (Fig. 5). In comparison to the symmetric D_{2h}-$(L_2Zr)_2(\mu\text{-}C{\equiv}CH)_2$ species, the distances of the metal centers to the C_α of the migrated alkynyl ligand change only slightly from 2.335 to 2.339 Å. However, there are significant changes in the alkynyl ligand π-conjugated to metal centers of the transition state with respect to the C_{2h}-$(L_2Zr)_2(\mu\text{-}C{\equiv}CH)_2$ isomer. In the TS, the following bonds shorten, Zr–C_α by 0.076 Å, Zr′–C_α by 0.083 Å, and Zr′–C_β by 0.105 Å, the C_α–C_β bond lengthens by 0.036 Å, indicating the dramatic change in the bonding interaction of the TS relative to C_{2h}-$(L_2Zr)_2(\mu\text{-}C{\equiv}CH)_2$. It appears that with the migration of a σ-alkynyl ligand of $(L_2Zr)_2(\mu\text{-}C{\equiv}CH)_2$, the major electron densities shift to the other alkynyl ligand by the Zr–alkynyl electron back donating interaction. Surprisingly, the stronger bonding interactions in the π-conjugated part of the transition state lead to a low migration barrier of 17.6 kcal/mol for the isomerization from the C_{2h}- to C_{2v}-$(L_2Zr)_2(\mu\text{-}C{\equiv}CH)_2$ isomers, which is significantly lower than half of the isomerization energy through the D_{2h}-$(L_2Zr)_2(\mu\text{-}C{\equiv}CH)_2$ transition structure. Taking thermal corrections into account, the calculated activation Gibbs free energy of 17.0 kcal/mol is consistent with the experimental value of 12–15 kcal/mol for the isomerization from the C_{2h}- to C_{2v}-$(L_2Zr)_2(\mu\text{-}C{\equiv}CH)_2$ isomers. Thus, our calculations suggest that the isomerization from the C_{2h}- to C_{2v}-$(L_2Zr)_2(\mu\text{-}C{\equiv}CH)_2$ isomers is slightly endothermic with a low barrier at room temperature.

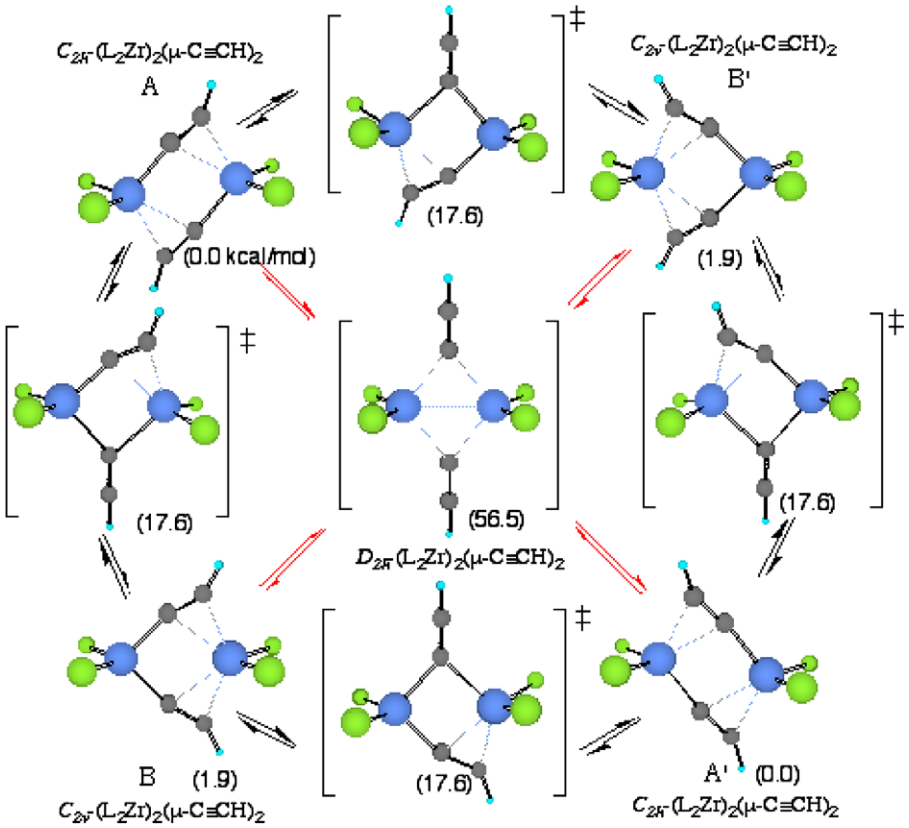

Fig. 4. The calculated energies and geometries of the isomerization and automerization processes of $(L_2Zr)_2(\mu\text{-}C{\equiv}CH)_2$.

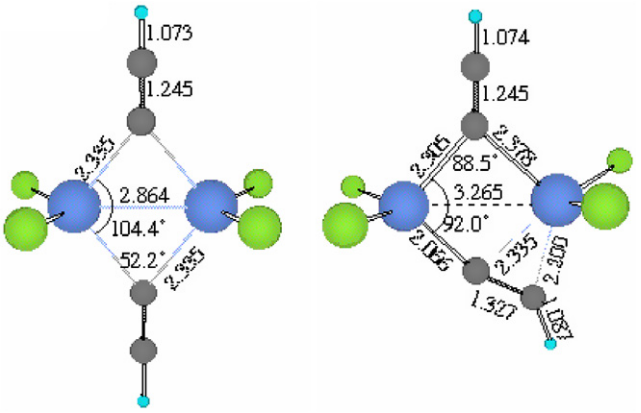

Fig. 5. The B3LYP optimized geometric parameters of the transition structures of the isomerization and automerization processes of $(L_2Zr)_2(\mu\text{-}C{\equiv}CH)_2$.

Overall, our calculations support that the automerization of both the C_{2h}- and C_{2v}-$(L_2Zr)_2(\mu\text{-}C{\equiv}CH)_2$ isomers proceeds along two isomerization processes, in which only one σ-alkynyl ligand is involved at a time, rather than along the symmetric D_{2h}-$(L_2Zr)_2(\mu\text{-}C{\equiv}CH)_2$ transition structure (Figs. 4 and 5). Because of the low activation energy, the isomerization of the C_{2h}- or C_{2v}-$(L_2Zr)_2(\mu\text{-}C{\equiv}CH)_2$ isomers appears to be a thermodynamically controlled process.

4. Conclusion

To elucidate the unique multi-center bonding network occurring in the doubly acetylide-bridged binuclear group 4 metallocene complexes and its role in the σ-alkynyl migration toward to C–C coupling/cleavage reactions of acetylides, DFT calculations were carried out on the bonding structure and σ-alkynyl migration mechanisms of the doubly acetylide-bridged binuclear Zr complexes $(L_2Zr)_2(\mu\text{-}C{\equiv}CH)_2$ $(L = Cp, Cl)$. The computational results were compared with the X-ray crystal structures and the results of the temperature-dependent dynamic NMR spectra.

The B3LYP calculations suggest that the reaction of $L_2Zr(C{\equiv}CH)_2$ with L_2Zr initially produces a C_{2v}-$(Cp'_2Zr)_2(\mu\text{-}C{\equiv}CH)_2$ complex, and then through a single σ-alkynyl ligand migration generates the C_{2h}-$(Cp'_2Zr)_2(\mu\text{-}C{\equiv}CH)_2$ isomer. In particular, the isomerization of the C_{2h}- or C_{2v}-$(L_2Zr)_2(\mu\text{-}C{\equiv}CH)_2$ isomers is almost thermoneutral through a low barrier of 15.3–17.0 kcal/mol, which can be regarded as an elementary step of automerization of the C_{2h}- or C_{2v}-$(L_2Zr)_2(\mu\text{-}C{\equiv}CH)_2$ complexes. Although the C_{2h}-$(L_2Zr)_2(\mu\text{-}C{\equiv}CH)_2$ isomer is slightly more stable than the C_{2v}-isomer at room temperature, the C_{2v}-$(L_2Zr)_2(\mu\text{-}C{\equiv}CH)_2$ may be thermodynamically favorable over the C_{2h}-isomer at higher temperature because the C_{2v}-isomer has slightly larger entropy relative to the C_{2h}-isomer. A careful transition state search ruled out the possibility of the automerization or isomerization directly through a symmetric D_{2h}-$(L_2Zr)_2(\mu\text{-}C{\equiv}CH)_2$ transition structure, which was confirmed to be a maximum with a high activation energy of 54–57 kcal/mol to link two isomers.

Overall, the MO orbital analysis indicated that the multi-center bonding interaction plays a very important role in the bonding structure and the σ-alkynyl migration of the doubly acetylide-bridged binuclear group 4 metallocene complexes. The MO Walsh diagram revealed that the C_{2h}- and C_{2v}-$(L_2Zr)_2(\mu\text{-}C{\equiv}CH)_2$ complexes have very similar multi-center bonding network structure, which can be attributed to a six-center-six-electron bonding pattern. The coplanar π-conjunction interaction through the electron donating and back-donating interactions between the metal centers and acetylide ligands significantly stabilizes the doubly acetylide-bridged binuclear group 4 metallocene complexes and the isomerization transition state. These results provide useful information in understanding the functions of the multi-center bonding network in the group 4 doubly acetylide-bridged binuclear complexes as well as corresponding C–C coupling processes.

Acknowledgements

We would like to thank the National Science Foundation (Grant No. CHE 9800184 and 0518024) and the Welch Foundation (Grant No. A-648) for their generous support. The partial calculations were performed at the EMSL, a national user facility sponsored by the US DOE's Office of Biological and Environmental Research and located at Pacific Northwest National Laboratory, operated for DOE by Battelle.

References

[1] R.H. Crabtree, The organometallic chemistry of the transition metals, third ed., John Wiley, New York, 2001.
[2] P. Nguyen, P. Gomez-Elipe, I. Manners, Chem. Rev. 99 (1999) 1515–1548.
[3] S.Q. Niu, M.B. Hall, Chem. Rev. 100 (2000) 353–405.
[4] I. Hylakryspin, S.Q. Niu, R. Gleiter, Organometallics 14 (1995) 964–974.
[5] R. Gleiter, I. Hylakryspin, S.Q. Niu, G. Erker, Organometallics 12 (1993) 3828–3836.
[6] G. Erker, D. Rottger, Angew. Chem., Int. Ed. Engl. 32 (1993) 1623–1625.
[7] G. Erker, M. Albrecht, C. Kruger, S. Werner, J. Am. Chem. Soc. 114 (1992) 8531–8536.
[8] R. Gleiter, I. Hylakryspin, S.Q. Niu, G. Erker, Angew. Chem., Int. Ed. Engl. 32 (1993) 754–756.
[9] D. Rottger, J. Pflug, G. Erker, S. Kotila, R. Frohlich, Organometallics 15 (1996) 1265–1267.
[10] D. Rottger, G. Erker, Angew. Chem., Int. Ed. Engl. 36 (1997) 813–827.
[11] J.H. Teuben, J. Organomet. Chem. 17 (1969) 87–93.
[12] G. Erker, W. Fromberg, R. Mynott, B. Gabor, C. Kruger, Angew. Chem., Int. Ed. Engl. 25 (1986) 463–465.
[13] G.L. Wood, C.B. Knobler, M.F. Hawthorne, Inorg. Chem. 28 (1989) 382–384.
[14] U. Rosenthal, H. Gorls, J. Organomet. Chem. 439 (1992) C36–C41.

[15] U. Rosenthal, A. Ohff, W. Baumann, R. Kempe, A. Tillack, V.V. Burlakov, Organometallics 13 (1994) 2903–2906.
[16] U. Rosenthal, A. Ohff, A. Tillack, W. Baumann, H. Gorls, J. Organomet. Chem. 468 (1994) C4–C8.
[17] U. Rosenthal, S. Pulst, P. Arndt, A. Ohff, A. Tillack, W. Baumann, R. Kempe, V.V. Burlakov, Organometallics 14 (1995) 2961–2968.
[18] N. Metzler, H. Noth, J. Organomet. Chem. 454 (1993) C5–C7.
[19] V. Varga, K. Mach, J. Hiller, U. Thewalt, P. Sedmera, M. Polasek, Organometallics 14 (1995) 1410–1416.
[20] A. Cano, T. Cuenca, M. Galakhov, G.M. Rodriguez, P. Royo, C.J. Cardin, M.A. Convery, J. Organomet. Chem. 493 (1995) 17–25.
[21] H. Lang, S. Blau, B. Nuber, L. Zsolnai, Organometallics 14 (1995) 3216–3223.
[22] F. Heshmatpour, S. Wocadlo, W. Massa, K. Dehnicke, Acta Crystallogr. Sect. C: Cryst. Struct. Commun. 51 (1995) 2225–2227.
[23] V.V. Burlakov, A. Ohff, C. Lefeber, A. Tillack, W. Baumann, R. Kempe, U. Rosenthal, Chem. Ber. 128 (1995) 967–971.
[24] P.M. Pellny, V.V. Burlakov, W. Baumann, A. Spannenberg, R. Kempe, U. Rosenthal, Organometallics 18 (1999) 2906–2909.
[25] P.M. Pellny, V.V. Burlakov, N. Peulecke, W. Baumann, A. Spannenberg, R. Kempe, V. Francke, U. Rosenthal, J. Organomet. Chem. 578 (1999) 125–132.
[26] P.M. Pellny, N. Peulecke, V.V. Burlakov, A. Tillack, W. Baumann, A. Spannenberg, R. Kempe, U. Rosenthal, Angew. Chem. Int. Ed. 36 (1997) 2615–2617.
[27] R. Gyepes, I. Cisarova, M. Horacek, J. Cejka, L. Petrusova, K. Mach, Collect. Czech. Chem. Commun. 65 (2000) 1248–1261.
[28] A. Spannenberg, F.G. Kirchbauer, V.V. Burlakov, U. Rosenthal, Z. Kristallogr. – New Cryst. Struct. 216 (2001) 619–620.
[29] V.V. Burlakov, P. Arndt, W. Baumann, A. Spannenberg, U. Rosenthal, P. Parameswaran, E.D. Jemmis, Chem. Commun. (2004) 2074–2075.
[30] N. Suzuki, T. Watanabe, M. Iwasaki, T. Chihara, Organometallics 24 (2005) 2065–2069.
[31] M. Horacek, P. Stepnicka, R. Gyepes, I. Cisarova, J. Kubista, L. Lukesova, P. Meunier, K. Mach, Organometallics 24 (2005) 6094–6103.
[32] S. Pulst, P. Arndt, B. Heller, W. Baumann, R. Kempe, U. Rosenthal, Angew. Chem., Int. Ed. Engl. 35 (1996) 1112–1115.
[33] G. Erker, W. Fromberg, R. Benn, R. Mynott, K. Angermund, C. Kruger, Organometallics 8 (1989) 911–920.
[34] Y. Raoult, R. Choukroun, D. Gervais, G. Erker, J. Organomet. Chem. 399 (1990) C1–C3.
[35] R.G. Parr, W. Yang, Density-Functional Theory of Atoms and Molecules, Oxford University Press, Oxford, 1989.
[36] A.D. Becke, J. Chem. Phys. 98 (1993) 5647–5648.
[37] C. Lee, W. Yang, R.G. Parr, Phys. Rev. B37 (1988) 785.
[38] P.J. Hay, W.R. Wadt, J. Chem. Phys. 82 (1985) 270–283.
[39] W.R. Wadt, P.J. HAY, J. Chem. Phys. 82 (1985) 284–298.
[40] P.J. Hay, W.R. Wadt, J. Chem. Phys. 82 (1985) 299–310.
[41] M. Couty, M.B. Hall, J. Comput. Chem. 17 (1996) 1359–1370.
[42] T.H. Dunning Jr., P.J. HayMethods of Electronic Structure Theory, vol. 2, Plenum Press, 1977.
[43] W.J. Hehre, R.F. Stewart, J.A. Pople, J. Chem. Phys. 51 (1969) 2657–2664.
[44] H.B. Schlegel, J. Comput. Chem. 3 (1982) 214–218.
[45] J.B. Foresman, A. Frisch, GAUSSIAN Inc., Exploring chemistry with electronic structure methods, second ed., Gaussian Inc., Pittsburgh, PA, 1996.
[46] M.J. Frisch, G.W. Trucks, H.B. Schlegel, G.E. Scuseria, M.A. Robb, J.R. Cheeseman, V.G. Zakrzewski, J.A. Montgomery, R.E. Stratmann, J.C. Burant, S. Dapprich, J.M. Millam, A.D. Daniels, K.N. Kudin, M.C. Strain, O. Farkas, J. Tomasi, V. Barone, M. Cossi, R. Cammi, B. Mennucci, C. Pomelli, C. Adamo, S. Clifford, J. Ochterski, G.A. Petersson, P.Y. Ayala, Q. Cui, K. Morokuma, D.K. Malick, A.D. Rabuck, K. Raghavachari, J.B. Foresman, J. Cioslowski, J.V. Ortiz, B.B. Stefanov, G. Liu, A. Liashenko, P. Piskorz, I. Komaromi, R. Gomperts, R.L. Martin, D.J. Fox, T. Keith, M.A. Al-Laham, C.Y. Peng, A. Nanayakkara, C. Gonzalez, M. Challacombe, P.M.W. Gill, B.G. Johnson, W. Chen, M.W. Wong, J.L. Andres, M. Head-Gordon, E.S. Replogle, J.A. Pople, Revision A., sixth ed., GAUSSIAN Inc., Pittsburgh PA, 1998.
[47] T.P. Straatsma, E. Aprà, T.L. Windus, E.J. Bylaska, W. de Jong, S. Hirata, M. Valiev, M. Hackler, L. Pollack, R. Harrison, M. Dupuis, D.M.A. Smith, J. Nieplocha, T.V., M. Krishnan, A.A. Auer, E. Brown, G. Cisneros, G. Fann, H. Früchtl, J. Garza, K. Hirao, R. Kendall, J. Nichols, K. Tsemekhman, K. Wolinski, J. Anchell, D. Bernholdt, P. Borowski, T. Clark, D. Clerc, H. Dachsel, M. Deegan, K. Dyall, D. Elwood, E. Glendening, M. Gutowski, A. Hess, J. Jaffe, B. Johnson, J. Ju, R. Kobayashi, R. Kutteh, Z. Lin, R. Littlefield, X. Long, B. Meng, T. Nakajima, S. Niu, M. Rosing, G. Sandrone, M. Stave, H. Taylor, G. Thomas, J. van Lenthe, A. Wong, Z. Zhang, NWChem, A Computational Chemistry Package for Parallel Computers, Version 4.6, Pacific Northwest National Laboratory, Richland, Washington 99352-0999, USA, 2004.
[48] R.A. Kendall, E. Apra, D.E. Bernholdt, E.J. Bylaska, M. Dupuis, G.I. Fann, R.J. Harrison, J.L. Ju, J.A. Nichols, J. Nieplocha, T.P. Straatsma, T.L. Windus, A.T. Wong, Comput. Phys. Commun. 128 (2000) 260–283.
[49] G. Black, B. Didier, T. Elsethagen, D. Feller, D. Gracio, M. Hackler, S. Havre, D. Jones, E. Jurrus, tT. Keller, C. Lansing, S. Matsumoto, B. Palmer, M. Peterson, K. Schuchardt, E. Stephan, H.T. Taylor, G., E. Vorpagel, T. Windus, C. Winters, Ecce, A Problem Solving Environment for Computational Chemistry, Software Version 3.2.1, Pacific Northwest National Laboratory, Richland, Washington 99352-0999, USA, 2004.
[50] W.E. Hunter, D.C. Hrncir, R.V. Bynum, R.A. Penttila, J.L. Atwood, Organometallics 2 (1983) 750–755.